Experimental quasiparticle dynamics in a superconducting, imaging x-ray spectrometer

S. Friedrich, K. Segall, M. C. Gaidis,[a] C. M. Wilson, and D. E. Prober[b]
Yale University, Department of Applied Physics, New Haven, Connecticut 06520-8284

A. E. Szymkowiak and S. H. Moseley
NASA Goddard Space Flight Center, Greenbelt, Maryland 20771

We present an experimental study of the time scales for various quasiparticle processes in a superconducting single photon spectrometer. Processes studied include quasiparticle recombination, diffusion, trapping, tunneling, and energy redistribution. Experiments were performed with a double junction, imaging x-ray detector whose charge output provides a measure of the photon energy. Time scales are extracted with a simple model and the values of several parameters, including the diffusion constant and recombination time, are found to differ from theoretical predictions. These results provide guidelines for performance analysis, device scaling, and future designs. © *1997 American Institute of Physics.* [S0003-6951(97)01852-4]

In recent years superconductors have been used in single photon spectrometers for x-ray photons and more recently for ultraviolet (UV) and visible photons.[1–4] A photon is absorbed in a superconductor, creating excess charge carriers (quasiparticles) which increase the subgap current of an attached tunnel junction. The integral of the increase in current, the charge, is proportional to the photon energy. Because of the small energy gap in the superconductor absorber these devices should have an excellent energy resolution for x rays, less than 5 eV full width at half maximum (FWHM) for a photon energy of 6 keV, more than 10× better than Si devices.[5] Experiments to date achieve a resolution of 29 eV.[1] Improved resolution and scaling to larger sizes are significant future goals. To achieve these goals it is important to better understand the device physics.

Operation of these devices differs from that of semiconductor devices in the means of charge transport and readout. In a semiconductor device, the charge is swept out and collected by an electric field. In a superconductor, the excitations travel by diffusion and are read out through a tunnel junction. Charge flow is controlled with band gap engineering. The quasiparticles are generated in the higher gap absorber (tantalum) and diffuse into a lower gap material, the trap (aluminum), where they scatter inelastically toward the gap energy of the trap. They then tunnel to the counter electrode. If two junctions are used with one absorber, the charge separation allows for one dimensional spatial resolution.[3,6]

Information on quasiparticle dynamics and energy redistribution is essential for proper design and for scaling to new designs in the future, especially for larger x-ray absorbers. Also, the theoretical value for the resolution is achieved only if each quasiparticle produced in the absorber is counted exactly once. This letter presents some of the first measurements and the most complete analysis to date of experimental quasiparticle dynamics issues in imaging superconducting detectors. We find unexpectedly slow diffusion in both Ta and Al and a recombination time in the Ta absorber which is shorter than that due to thermal recombination alone. In ad-

dition, the trapping efficiency and the dependence of the charge on bias voltage can be understood from the quasiparticle inelastic scattering rate in the two Al junction electrodes; this rate agrees with the theoretical prediction for Al.

The samples studied have a double-junction geometry, shown in Fig. 1. A Ta film (Δ_{Ta}=0.7 meV) 6000 Å thick forms the absorber. Each trap is an Al film, 1500 Å thick. X rays absorbed in the Ta break Cooper pairs, creating excess quasiparticles which cool in about 100 ps to near the Ta gap edge, over a distance of about 3 μm.[7] They then diffuse at this energy, and, after reaching either trap, scatter down inelastically toward the Al gap energy (Δ_{Al}=0.18 meV) and tunnel to the counter electrode. Each junction is voltage biased in the subgap region. The charge for each junction is found by numerically integrating the digitized current wave form. The sum of the two quasiparticle charges is proportional to the photon energy. Their ratio determines the absorption location. With no loss, a plot of the charge from the two junctions, Q_1 vs Q_2, would be a straight line for fixed
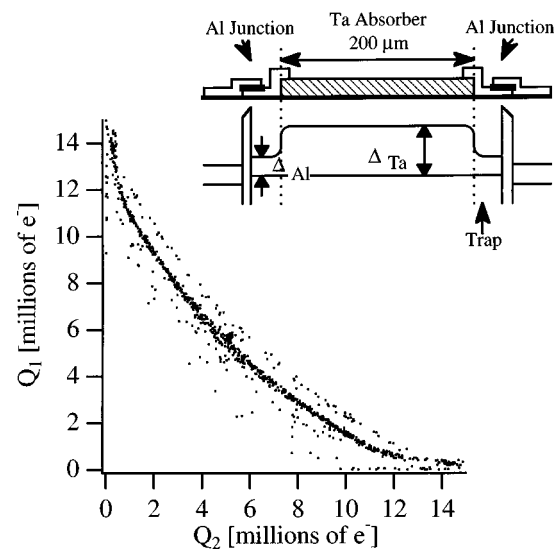

FIG. 1. Charge collected in junction 1 vs charge collected in junction 2 for the Ta device (T=0.23 K, V=70 μV). The curvature of the data is due to a finite loss time in the absorber. Cluster of points at $Q_1=Q_2=5.5$ million electrons is from electronically injected current pulses. Inset shows the device schematic along with the energy diagram for the different films.

TABLE I. Summary of results; values for times are from experiment.

Device	$D[\text{cm}^2/\text{s}]$ (theory)	$D[\text{cm}^2/\text{s}]$ (experiment)	$\tau_{\text{loss}}[\mu\text{s}]$	$\tau_{\text{trap}}[\mu\text{s}]$	$\tau_0[\mu\text{s}]$
Ta	40	8	31	<0.01	0.44
Ta/Al	530	60	1	8	$\cdots$

FIG. 2. Delay time vs absorption location for the Ta device ($T=0.23$ K, $V=70\ \mu$V), for two different values of threshold current. The solid lines are fits from the model. The inset shows the onset of a set of pulses, one from each junction, from a single x-ray. (The larger pulse is cut off.) The time delay is clearly visible.

photon energy.[8] The plot of Q_1 vs Q_2 in Fig. 1 is for an x-ray source with a dominant emission at 5.9 keV and a weaker emission at 6.5 keV. Experiments were done at $T=0.23–0.33$ K. Details of device fabrication and electronic readout have been published.[2,6]

The device shown in the inset of Fig. 1 is the Ta device; we have tested two of these. The energy gap diagram is shown for the different films. We have also tested another device, the Ta/Al device, in which the Al trap overlays the entire absorber. In this latter device the x rays are also absorbed in the Ta, due to its high atomic number. However, the quasiparticles are trapped vertically into the lower gap Al overlayer and diffuse laterally in the Al. Trapping does occur in this Ta/Al device because the gap of the Al overlayer is increased above that of the Al trap by proximity effect with the Ta.

To extract the relevant time scales from the measurements, we employ a numerical model of the current pulses. After the 100 ps of initial cooling, we treat the quasiparticle propagation with the one-dimensional diffusion equation. We include a loss time, τ_{loss}, to account for recombination in the absorber. Trapping is simulated by the boundary condition $D(\partial n/\partial x)|_{x=\pm L/2}=n|_{x=\pm L/2}(D\tau_{\text{trap}})^{-1/2}$ at the absorber/trap interface with $n(x)$ the density of quasiparticles, D the diffusion constant in the absorber, and L the length of the absorber (200 μm).[9] The value τ_{trap} represents the average time it takes a quasiparticle to be trapped; for perfect trapping ($\tau_{\text{trap}}\rightarrow 0$) the relation becomes $n|_{x=\pm L/2}=0$. Tunneling and inelastic scattering in the Al electrodes are treated by a system of rate equations for the energy distribution of quasiparticles.[10] The parameters in this simulation are Q_0 (the initial quasiparticle charge), D, τ_{tunn} (the tunnel time in the normal state[11]), τ_{loss}, and τ_{out} (the time to diffuse in the Al counter electrode away from the junction area). These parameters are determined in separate measurements. The simulated current pulses fit the digitized wave forms well.

Losses in the absorber give the curvature of the Q_1 vs Q_2 plot, Fig. 1, since quasiparticles created in the center have to diffuse a longer distance (time) before being trapped. We find $\tau_{\text{loss}}=31\ \mu$s in the Ta device and $\tau_{\text{loss}}\approx 1\ \mu$s in the Ta/Al device, listed in Table I. (The values for D are discussed below.) The loss times are independent of temperature. For Ta, τ_{loss} is smaller than the value of 2800 ms due to thermal recombination alone.[14] We speculate that the loss is due to trapping sites in the film, either at the surfaces or due to magnetic flux penetration. Our calculations show that a small, perpendicular magnetic field (~ 1 G) could explain the short loss time. A magnetic field of about 15 G is applied *parallel* to the film in order to suppress the Josephson current, but may have a small perpendicular component due to imperfect alignment.

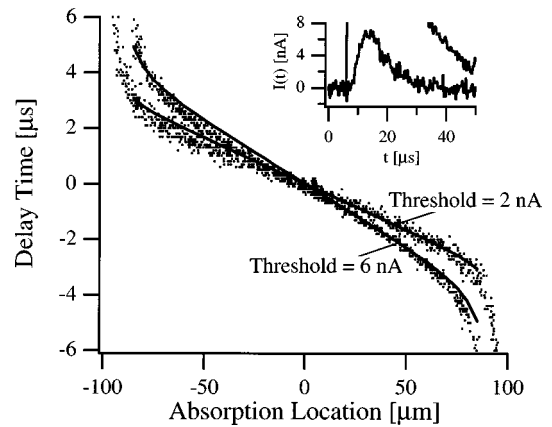We determine the diffusion constant in the absorber film

from the difference in arrival times of the current pulses in the two junctions, at a specific current threshold (see inset, Fig. 2). Figure 2 shows the delay time versus absorption location for the Ta device. The data are compared with results from the simulation. A best fit is obtained for $D_{\text{Ta}}=8$ cm^2/s (solid line), and is insensitive to the threshold chosen. This value is much lower than we calculate using the low temperature resistivity of our Ta, 0.48 $\mu\Omega$ cm. We calculate a value for the normal state of $D_n=180$ cm^2/s.[12] D is reduced in the superconducting state because the quasiparticle dispersion relation has a minimum at the gap edge where the group velocity is zero.[13] The degree of reduction depends on how close to the Ta gap edge the quasiparticles relax. Simulation shows that within 0.2 μs the quasiparticles relax to a distribution with an effective value of $D=40$ cm^2/s, but that D decreases very little after that (during the time for a typical current pulse). Thus, there is a factor of 5 disagreement between theory, $D_{\text{Ta}}=40$ cm^2/s, and experiment, $D_{\text{Ta}}=8$ cm^2/s. For the Ta/Al device a similar discrepancy exists, with the experimental value of $D_{\text{Al}}=60$ cm^2/s, compared to a prediction of $D_{\text{Al}}=530$ cm^2/s. The measured values are independent of temperature over the range studied.

Trapping occurs when the quasiparticles scatter inelastically to lower energy in the Al trap regions. The rate of trapping can be determined from the Q_1 vs Q_2 plots by focusing on events close to one junction. If the scattering is fast, quasiparticles are trapped immediately and the charge in the opposite junction is nearly zero. If the trapping is slow, quasiparticles diffuse back to the absorber and cause a finite charge in the other junction. Thus, with slow trapping the charge separation is weak and the points cluster toward the center of the plot of Q_1 vs Q_2.

The Ta device shows fast trapping and effective charge separation. The data can be fit with a trapping time $\tau_{\text{trap}}<10$ ns. This agrees well with the predicted trapping time of 6 ns for injection at the Ta gap energy into the Al. This 6 ns time is derived from an inelastic parameter $\tau_0=0.44\ \mu$s computed for Al.[14] The Ta/Al device shows weaker charge separation because the gap in the Al overlayer is not strongly enhanced (by proximity effect with the Ta), as
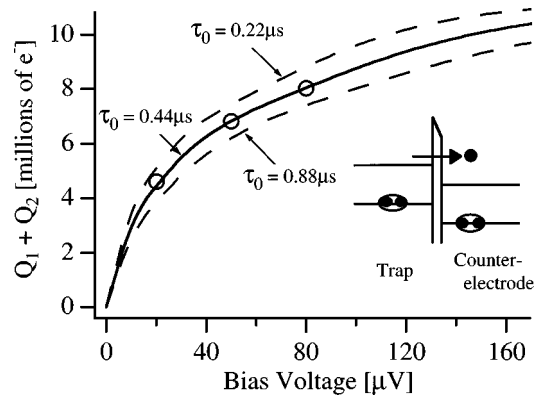
Friedrich *et al.*

FIG. 3. Total charge, $Q_1 + Q_2$, vs bias voltage for the Ta device ($T = 0.23$ K). The circles are experimental data and the lines are fits from the model for different values of τ_0. Inset shows the energy diagram with an allowed forward tunneling process. The reduction in charge at low bias is due to cancellation of the forward current by reverse processes.

compared with the gap in the Al trap. The fitted trapping time is 8 μs. We do not have sufficient information on the gap in the Al overlayer to predict τ_{trap} for the Ta/Al device.

Another measure of the inelastic scattering in the Al trap is the dependence of the charge on temperature. We can fit the temperature dependence of the charge using the same value of τ_0 which was consistent with the measured trapping time.

The charge output also depends on bias voltage. This can be understood as partial cancellation of the forward tunneling processes by reverse processes. Consider the simplified case where the quasiparticles in the counter electrode do not diffuse away from the junction. A quasiparticle which has tunneled into the counter electrode can tunnel back to the trap and ''cancel'' the forward current if its energy in the counter electrode has not relaxed to below the gap of the Al trap. (See Fig. 3 inset; allowed tunneling in this diagram is horizontal.) Once a quasiparticle in the counter electrode has relaxed its energy below the gap in the trap, however, it cannot tunnel back and cancel the forward current. Thus, if the inelastic scattering to lower energy in the counter electrode is rapid, the reverse current will be small and there will be little cancellation.[15] This is the case for large bias voltages, V, since the inelastic scattering rate due to phonon emission is large (scaling approximately like V^3).[14] For smaller bias voltages, however, the inelastic scattering is weaker so the reverse current is larger and the total charge is reduced. Fast diffusion of quasiparticles away from the tunnel barrier into the leads would reduce the amount of reverse tunneling; however, because the diffusion is slow in the Al counter electrode the outdiffusion time, τ_{out}, is comparable to the back tunneling time.

We plot in Fig. 3 the charge collected for events in the center of the absorber versus bias voltage, and also fit this with our simulation. The value of τ_0, the inelastic parameter for Al, is used as a fitting parameter. The solid curve is for $\tau_0 = 0.44$ μs. The two dashed curves are for τ_0 values two times smaller and two times larger. The general agreement seen demonstrates that quasiparticle relaxation and reverse processes determine the voltage dependence of the charge in these devices. The data can be fit with the theoretical value

of $\tau_0 = 0.44$ μs. This agreement, and its consistency with the temperature dependence of the total charge and the trapping time, provide a check on the self-consistency of our approach, besides giving an estimation of the value of τ_0 itself.

We conclude that the physical models we have developed describe well the device operation: gain, time scales, and trapping. Issues of noise remain to be resolved in future work. The measured parameters (see table) show that scaling to millimeter sizes, as desired for astrophysical x-ray detectors, is feasible. With a loss time of 31 μs, an absorber 1 mm in size would still achieve an energy resolution the same as at present, provided the electronic noise can be reduced to 1200 electrons FWHM.[2] For new designs, a lower limit on absorber and trap size can also be computed from our model with these parameters, to ensure efficient charge separation and trapping.[3] This is relevant to the UV/visible photon detectors, where small pixels and large count rates are anticipated. Finally, for the charge to be less dependent on bias voltage, a bias voltage above 120 μV is desirable.[16]

[1] M. Frank, C. A. Mears, S. E. Labov, F. Azgui, M. A. Lindemann, L. J. Hiller, H. Netel, and A. Barfknecht, Nucl. Instrum. Methods Phys. Res. A **370**, 41 (1996).

[2] S. Friedrich, K. Segall, M. C. Gaidis, C. M. Wilson, D. E. Prober, P. J. Kindlmann, A. E. Szymkowiak, and S. H. Moseley, IEEE Trans. Appl. Supercond. **7**, 3383 (1997).

[3] H. Kraus, F. V. Freilitzsch, J. Jochum, R. L. Mossbauer, T. Peterreins, and F. Probst, Phys. Lett. B **321**, 195 (1989).

[4] P. Verhoeve, N. Rando, A. Peacock, A. van Dordrecht, and A. Poelaert, IEEE Trans. Appl. Supercond. **7**, 3359 (1997).

[5] M. Kurakado, Nucl. Instrum. Methods Phys. Res. A **196**, 275 (1982). For a Ta absorber, a resolution of 3 eV FWHM is predicted.

[6] S. Friedrich, K. Segall, D. Toledano, D. E. Prober, A. E. Szymkowiak, and S. H. Moseley, Nucl. Instrum. Methods Phys. Res. A **370**, 44 (1996); M. C. Gaidis, S. Friedrich, D. E. Prober, A. E. Szymkowiak, and S. H. Moseley, J. Low Temp. Phys. **93**, 603 (1993).

[7] S. Friedrich, Ph.D. thesis, Yale University, 1997.

[8] The points at lower energy in Fig. 1 are due to substrate absorptions.

[9] J. Jochum, H. Kraus, M. Gutsche, B. Kemmather, F. V. Freilitzsch, and R. L. Mossbauer, Ann. Phys. (Leipzig) **2**, 611 (1993).

[10] We divide up the energies in the trap/counter electrode into bins of 10 μV and calculate the number of quasiparticles entering/leaving each bin through inelastic scattering, tunneling, recombination or outdiffusion. Both scattering and tunneling rates are energy dependent (see Refs. 6, 7, 11, and 14).

[11] The tunneling time in the normal state is calculated from the resistivity of the barrier. In the superconducting state, the tunnel time is shorter for quasiparticle energies near the gap edge because of the larger density of states (see Ref. 8). This is accounted for in the model.

[12] The Einstein equation $D = 1/[\rho n(E_F)e^2]$ relates the resistivity, ρ, to the diffusion constant with a minimum number of band-structure dependent quantities; $n(Ef)$ is the density of states at the Fermi surface.

[13] V. Narayanamurti, R. C. Dynes, P. Hu, H. Smith, and W. F. Brinkman, Phys. Rev. B **18**, 6041 (1978).

[14] S. B. Kaplan, C. C. Chi, D. N. Langenberg, J. J. Chang, S. Jafarey, and D. J. Scalapino, Phys. Rev. B **14**, 4854 (1976).

[15] There is a second process, called back tunneling, which gives a current in the forward direction: a pair splits in the trap, and coherently one electron from that pair forms a pair in the counter electrode. Here also there is a reverse process which cancels the forward current at low voltage.

[16] Our present devices are limited to the voltage range $V < 90$ μV by Fiske modes. With a smaller junction length, biasing at higher voltages will be easily accomplished.

Appl. Phys. Lett., Vol. 71, No. 26, 29 December 1997

Friedrich et al. 3903